Pis'ma v ZhETF, vol. 102, iss. 6, pp. 361 – 365

Scaling and asymptotic properties of evaporated neutron inclusive cross sections in high energy hadron-nucleus and nucleus-nucleus interactions

A. S. Galoyan[+], *A. Ribon*[*], *V. V. Uzhinsky*[×1)]

[+] *Veksler and Baldin Laboratory of High Energy Physics, Joint Institute for Nuclear Research, 141980 Dubna, Russia*

[*] *Conseil Européen pour la Recherche Nucléaire, 1211 Genèva, Switzerland*

[×] *Laboratory of Information Technologies, Joint Institute for Nuclear Research, 141980 Dubna, Russia*

Submitted 13 May 2015

Resubmitted 10 August 2015

New properties of the evaporated neutron ($E < 30$ MeV) energy spectra in hadron-nucleus interactions are found which have not been marked before. Particularly, the spectra approach the asymptotic regime, namely, they weakly depend on the collision energy at momenta of projectile protons larger than 5–6 GeV/c; the spectra for various nuclei are similar, and can be approximately described by the function $A^n f(E)$. Experimental data on neutron spectra in the case of projectile π-mesons show analogous behaviour, but the statistics of the data do not allow one to draw clear conclusions. In our analysis we used ITEP experimental data on inclusive cross sections of neutrons produced in interactions of π-mesons and protons with various nuclei in the energy range from 747 MeV up to 8.1 GeV. The observed properties allow one to predict neutron yields in the nucleus-nucleus interactions at high and super high energies. Predictions for the NICA/MPD experiment at JINR are presented. It is shown that the FTF (Fritiof)-model of the Geant4 toolkit qualitatively reproduces the observed regularities. For the first time estimates of the neutron energy flows are obtained at both RHIC and LHC energies.

DOI: 10.7868/S0370274X15180022

Neutron and proton production in high energy nuclear reactions has been studied for a long time. The relevant research was mainly devoted to checking a nuclear scaling hypothesis [1–3] that the inclusive cross sections of sufficiently energetic nucleons in the target fragmentation region are independent of the incident projectile particle type and energy as well as their shapes on the target nucleus at sufficiently high energies (see also reviews [4–7]). Thus far, no scaling properties of the low energy part of the nucleon kinetic energy spectra have been considered. When studying the experimental data [8] obtained at the Moscow Institute for Theoretical and Experimental Physics (ITEP), we noted that slow neutron spectra had interesting regularities.

Protons, π^+ and π^- mesons were used as projectiles in the ITEP experiments over a wide energy range. Some results were published in [2, 9]. Summary tables[2)] were presented in an ITEP preprint [8]. In Fig. 1 we show sampling data from the tables [8] on the inclusive neutron production cross section on a lead target at emission angle 119°.

It is known that the neutron spectra have a two-component structure. Evaporated neutrons dominate at energies below 30 MeV. Pre-equilibrium neutrons or neutrons participating in the fast stage of reactions dominate at higher energies. According to the data, the fast neutron spectra are weakly energy-dependent at $P_{\rm lab} > 5{-}6$ GeV/c. The low-energy parts of the spectra, shown in the figure, have the same behaviour – they are approaching the asymptotic regime at $P_{\rm lab} > 5$ GeV/c.

Since it is complicated to deal with all various distributions, let us study the behaviour of the slow neutron spectra looking at the energy and target mass dependencies of the inclusive cross sections at neutron kinetic energies $T = 8.5$, 11, and 15 MeV. We think that at these energies the data represent the main properties of the slow neutron spectra. The corresponding experimental data for C, Cu, and Pb targets are presented in Fig. 2.

As seen especially for the lead and copper nuclei and proton projectiles, the asymptotic behaviour takes place at $P_{\rm lab} \sim 5{-}6$ GeV/c. The data for $p + {\rm C}$ reactions presented in [8] only for $P_{\rm lab} \geq 6$ GeV are poorer, and not sufficient to draw the same conclusion. Thus, the approaching of the asymptotic regime seems to be inde-

1) e-mail: uzhinsky@jinr.ru

2) We have checked the consistency of the data [8] against more modern data of the paper [10].

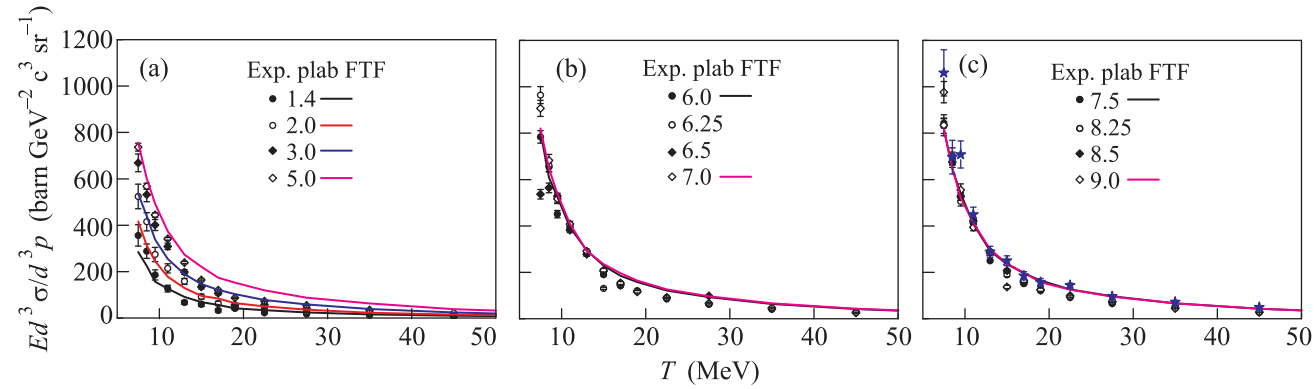

Fig. 1. Inclusive neutron production cross sections in $p+$Pb interactions at various projectile momenta: 1.4, 2, 3, and 5 GeV/c (a); 6, 6.25, 6.5, and 7 GeV/c (b); 7.5, 8.25, 8.5, and 9 GeV/c (c). Points are experimental data [8]. Lines are FTF model calculations

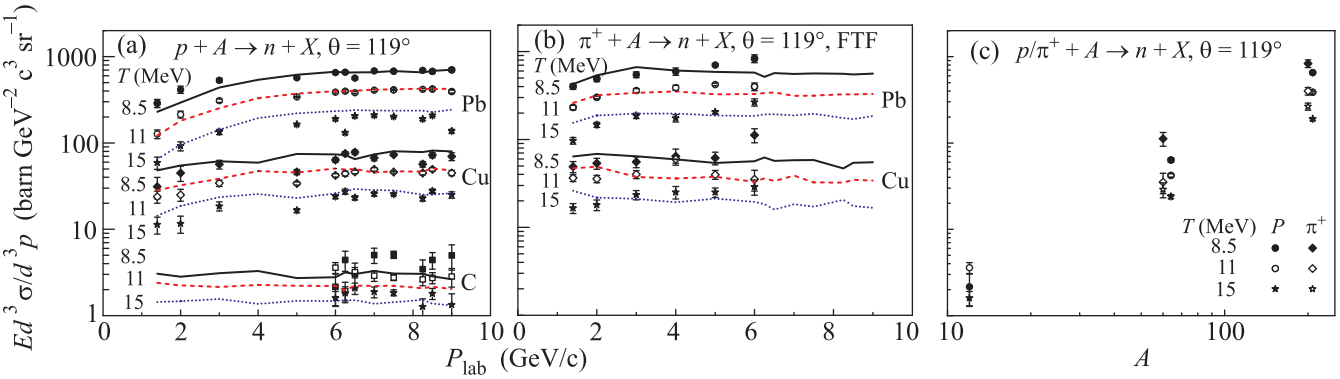

Fig. 2. (a, b) – Inclusive neutron production cross sections in $p + A$ and $\pi^+ + A$ interactions at various projectile momenta and $\theta = 119°$. Points are experimental data [8]. Lines are FTF model calculations. Solid, dashed, and dotted lines represent the calculated cross sections at neutron kinetic energies 8.5, 11, and 15 MeV, respectively. (c) – Experimental cross sections for $p + A$ and $\pi^+ + A$ interactions [8] only at $P_{lab} = 6$ GeV/c. The points for $\pi^+ + A$ interactions are shifted to the left for clarity

pendent of the target nucleus, at least for medium and heavy nuclei.

A more complicated situation takes place for $\pi + A$ cross sections (see Fig. 2b). According to our point of view, the data at $P_{lab} = 6$ GeV/c do not fit the pattern. The data for $\pi^+ +$ Pb interactions at $P_{lab} < 3$ GeV/c decrease faster with energy decreasing than the data for $\pi^+ +$Cu interactions. Our calculations deviate more from the data for $\pi^+ +$ Cu interactions than from the data for $\pi^+ +$ Pb interactions in this energy range. However, it seems that the approach to asymptotic behaviour for $\pi+A$ interactions starts earlier than for $p+A$ collisions. To make a conclusion in this case, one needs data at projectile momenta lower than 1 GeV/c.

According to the nuclear scaling hypothesis, the inclusive cross sections of fast nucleons scale as A^n. Looking at Fig. 2c, one can see that the scaling coefficient depends on the kinetic energy of the evaporated neutron and on the projectile type, at least at $P_{lab} = 6$ GeV/c where the data for pA and πA interactions are presented in [8]. Thus, we can say that nuclear scaling is only approximate for evaporated neutrons, and we consider the title of our paper to be a question for further experimental and theoretical studies.

It is usually assumed that the slow nucleons are produced during the relaxation of the equilibrated nuclear residuals, and various intra-nuclear cascade models are successfully applied for simulation of the production. The models simulate the fast stage of the reaction. Subsequently, 4-momenta of produced fast particles are summed, and the excitation energies of residual nuclei are calculated using energy-momentum balance. Thus, the asymptotic behaviour of the spectra can reflect asymptotic properties of hadron-nucleon interactions or a space-time structure of the production process, such as the formation time of produced particles. It

is complicated to consider the asymptotic properties of hadron-nucleon interactions at energies below 10 GeV. The formation time concept was criticized in [11] from the view point of reggeon field theory. The method of the excitation energy calculations given above cannot be applied to nucleus-nucleus interactions and it is likely that there are additional problems. In many Monte Carlo models for the simulation of hadron-nucleus interactions a transition from the low energy cascade models to the high energy quark-gluon models occurs at $P_{\rm lab} \sim 4{-}6\,\mathrm{GeV/c}$. For example, in the Geant4 toolkit the transition between the low energy Bertini-like cascade model (BERT) and the high energy FTF (Fritiof) model [12, 13] is implemented. As shown by the HARP-CDP experimental group [14], the transition leads to irregularities which are not confirmed by experiment. In order to clarify the problem and interpret our observations, we chose the Geant4 FTF model in which the transition is presented in an implicit form.

The FTF model originates from the well-known Fritiof model [15, 16]. It considers the creation and fragmentation of quark-gluon strings in hadronic interactions. The simplified Glauber approach is applied at the beginning of the FTF code to determine the participating nucleons in hadron-nucleus and nucleus-nucleus interactions[3)]. After that string creation and fragmentation are simulated. The reggeon theory inspired model of nuclear destruction (RTIM) [18, 19] is used for the calculation of nuclear remnant properties and the simulation of the pre-equilibrium nucleon production[4)]. Reggeon theory inspired model assumes that the spectator nucleons can be involved by the participating ones at the first stage of the interaction. The probability to involve a spectator nucleon having coordinates in the impact parameter plane $\mathbf{b}_i$ by a participating nucleon with coordinates $\mathbf{b}_j$ is written as

$$P_{ij} = C_{nd} e^{-|\mathbf{b}_i - \mathbf{b}_j|^2/R^2}, \quad R \simeq 1.2\,\mathrm{fm}, \tag{1}$$

$$C_{nd} = 0.00481 A e^{4(y_p-2.1)}/(1+e^{4(y_p-2.1)}). \tag{2}$$

Here, A is the mass number of the target nucleus and y_p is the rapidity of the projectile in the target nucleus rest frame.

A quite complicated algorithm [21, 22] for ascribing the momenta to the involved and participating nucleons is used in the FTF model. Simplifying the exact expressions, we can say that the particle momentum distribution is given by

$$P(p_z, \mathbf{p}_T) \propto e^{-|\mathbf{p}_T|^2/\langle|\mathbf{p}_T|^2\rangle} e^{-(x^- - 1/N_N)^2/(0.3/N_N)^2},$$

$$x^- = (E - p_z)/(E_N - P_N), \tag{3}$$

$$\langle|\mathbf{p}_T|^2\rangle = 0.035 + 0.04 e^{4(y_p-2.5)}/(1+e^{4(y_p-2.5)})\ (\mathrm{GeV/c})^2. \tag{4}$$

Where N_N is the multiplicity of the involved and participating nucleons, x^- is the light-cone momentum fraction, E_N and P_N are the re-defined energy and momentum of the interacting nucleons of the target nucleus (see [21, 22]). All numbers in Eqs. (1)–(4) were determined in order to reproduce the HARP-CDP group experimental data [23].

The reggeon theory inspired model (RTIM) of nuclear destruction is used in our calculations instead of a standard intra-nuclear cascade model starting from $P_{\rm lab} \sim (1.2{-}1.4)\,\mathrm{GeV/c}$. Thus, we have no transition between models going from low to high energies.

The FTF model uses a method proposed in [24] to calculate the excitation energies. It is assumed that each involved or participating nucleon contributes to the excitation energy, Δe, distributed according to the law:

$$P(\Delta e) = e^{-\Delta e/\langle\Delta e\rangle}/\langle\Delta e\rangle. \tag{5}$$

We found that a good description of the ITEP data presented above (see Fig. 1, solid curves) required that $\langle\Delta e\rangle \simeq 40\,\mathrm{MeV}$. This value also gives satisfactory results for the πA interactions (see Fig. 2). The data [10] on the pA reactions at the energies of 800, 1200, and 1600 MeV are described by $\langle\Delta e\rangle \simeq 40\,\mathrm{MeV}$ as well.

It is important to note that Eqs. (2) and (4) describe a smooth transition from low to high energies. The center of the transition region for the pA interactions determined by $y_p = 2.1$ corresponds to $P_{\rm lab} \simeq 3.8\,\mathrm{GeV/c}$. The analogous value for the πA interactions is $570\,\mathrm{MeV/c}$. Such a difference between πA and pA interactions is represented in the data (see Figs. 2a and 2b, respectively). We expect that the center of the transition region for kaon-nucleus interactions will be located at intermediate values of the projectile momenta.

As seen in Figs. 1 and 2, the FTF model with tuned parameters qualitatively reproduces the observed regularities of the cross sections. The increase of the slow neutron yield with the energy growth (see Fig. 2) at $P_{\rm lab} \sim 1.4{-}4\,\mathrm{GeV/c}$ is connected with increasing the nuclear destruction which is regulated by Eqs. (1) and (2) and reflects the growth of the reggeon cascading.

To check the applicability of the FTF model to nucleus-nucleus interactions let us turn to experimental data on $\mathrm{C} + A$ interactions at 2 GeV/nucleon [25].

[3)] A more advanced Glauber code is presented in [17].

[4)] Recently [20] RTIM was coupled with the HIJING model which gives additional opportunities to design high energy experiments.

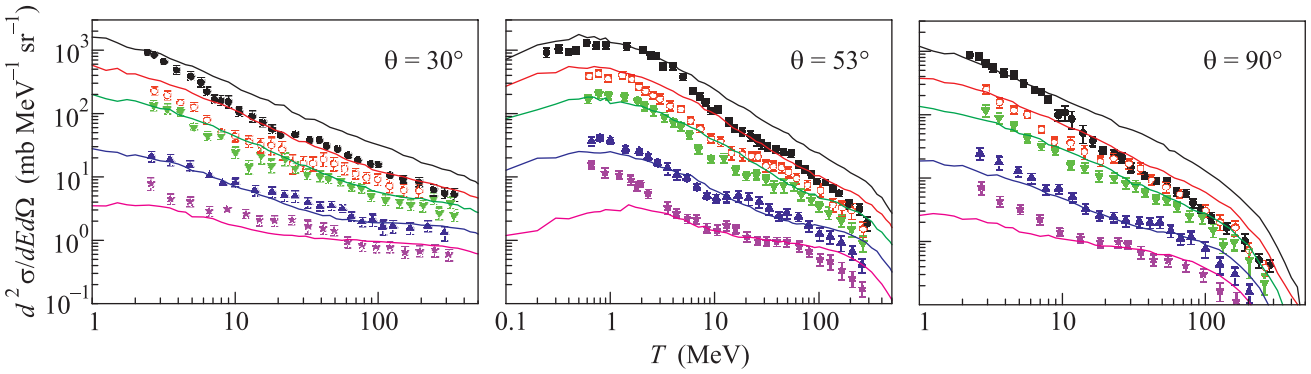

Fig. 3. (Color online) Inclusive cross sections of neutron production in C + Pb, Cd, Cu, Al, C interactions at 2 GeV/nucleon (from top to bottom). Points are experimental data [25]. Lines are our calculations

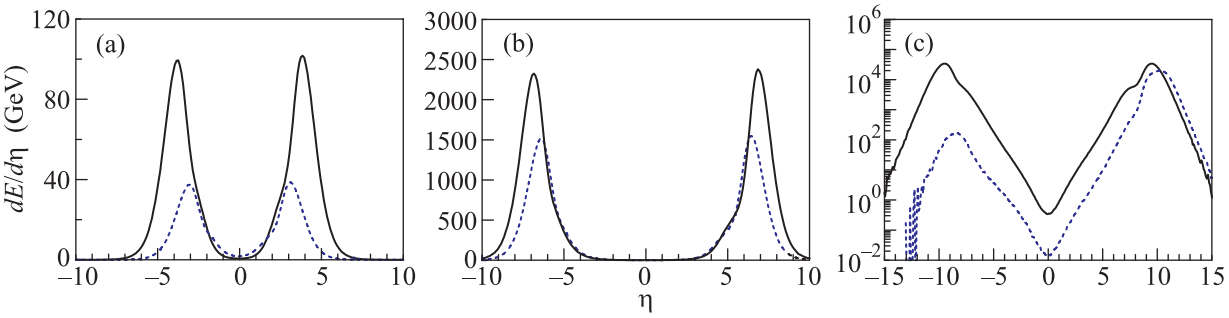

Fig. 4. Calculation of neutron kinetic energy flows in nucleus-nucleus interactions

In Fig. 3 we present the experimental data and our calculations with the improved FTF model. The model is seen to reproduce the experimental data, except for the neutron yield in C + Pb interactions at $T > 7$ MeV. The source of the disagreement is now under study. The data on p, d, α+Pb interactions [26], not shown in our paper, are described quite satisfactorily. Thus, it is hoped that the FTF model will give reliable predictions at other energies.

One of the important applications of the model is the estimation of neutron flow in nucleus-nucleus interactions at high energy accelerators. Fig. 4 presents our calculations of the neutron kinetic energy flows at RHIC (BNL, USA) and LHC (CERN, Geneva) as well as for the future NICA facility (JINR, Dubna). Fig. 4a gives the flows for Au + Au interactions at the nucleon-nucleon CMS energies, $E_{\rm CMS}$, of 5 and 10 GeV, which are planned for investigation at NICA (dashed and solid lines correspondingly). Fig. 4b shows the flows in Au + Au collisions at RHIC for $E_{\rm CMS}$ = = 130 and 200 GeV (dashed and solid lines, correspondingly). The results for LHC (Pb + Pb and p + Pb collisions at $E_{\rm CMS} = 2760$ and 5020 GeV (solid and dashed lines, respectively) are presented in Fig. 4c. The flows are calculated as functions of pseudo-rapidity – η = $= -\ln[{\rm tg}(\theta/2)]$, where θ is the angle between the beam direction and the flow direction. Using these calculations, one can estimate the radiation dose of various detectors and equipment. Phenomenological models are usually applied for such estimates.

Other applications such as radiation damage in organic materials and electronic devices may also be considered within the proposed approach.

It should be noted that colliding beams are used at LHC and RHIC, and will be used at NICA. The beams circulate in opposite directions. At the LHC, each of the beams had 1380 GeV/nucleon for Pb + Pb collisions. For p + Pb collisions, the beam of the lead nuclei had 1577 GeV/nucleon, and the proton beam had an energy of 4000 GeV. These resulted in $E_{\rm CMS} = 5020$ GeV. The neutron distribution in η is asymmetric for the p + Pb collisions. The neutron yield from the lead nuclei remnants at $\eta > 0$ is larger than the yield in the proton fragmentation region (see dashed line in Fig. 3c). Since the lead nuclei had almost the same energies for PbPb and pPb collisions, $dE/d\eta$ distributions are quite close at $\eta > 10$ (see Fig. 3c). The difference between the distributions at $\eta < 10$ is caused by the different excitation energies of the remnants. This can be checked by experiment.

Finally, we would like to say that all the results presented in this paper can be reproduced using the FTFP_BERT physics list in Geant4 release G4_10.2 which will be available in early December, 2015. A test version of the release (G4_10.2.beta) became available to the public in late July, 2015.

The authors of the paper are grateful to the Geant4 hadronic working group for interest in the work and especially for support provided by G. Folger, V.I. Ivanchenko, and A. Howard. The authors are thankful to V.I. Yurevich, A.G. Litvinenko, and V.S. Stavinsky for their useful consideration of the research issue.

1. Yu. D. Bayukov et al., Yad. Fiz. **18**, 1246 (1973) [Sov. J. Nucl. Phys. **18**, 639 (1974)].
2. Yu. D. Bayukov et al., Yad. Fiz. **19**, 1266 (1974) [Sov. J. Nucl. Phys. **19**, 648 (1974)].
3. G. A. Leksin, *Transactions of the 18th International conference on high energy Physics*, Tbilisi (1976), v. 1, A6-3.
4. V. S. Stavinsky, Sov. J. Part. Nucl. **10**, 468 (1979) [Fiz. Elem. Chast. Atom. Yadra **10**, 949 (1979)].
5. V. K. Lukyanov and A. I. Titov, Sov. J. Part. Nucl. **10**, 334 (1979) [Fiz. Elem. Chast. Atom. Yadra **10**, 815 (1979)].
6. L. L. Frankfurt and M. I. Strikman, Phys. Rept. **76**, 215 (1981).
7. A. M. Baldin, Fiz. Elem. Chast. Atom. Yadra **8**, 429 (1977).
8. Yu. D. Bayukov et al., ITEP preprint # 172 (1983).
9. Yu. D. Bayukov et al., Yad. Fiz. **42**, 377 (1985) [Sov. J. Nucl. Phys. **42**, 238 (1985)].
10. S. Leray et al., Phys. Rev. C **65**, 044621 (2002).
11. K. G. Boreskov, A. B. Kaidalov, S. M. Kiselev, and N. Ya. Smorodinskaya, Yad. Fiz. **53**, 569 (1991) [Sov. J. Nucl. Phys. **53**, 356 (1991)].
12. V. Uzhinsky, *Proc. Intern. Conf. on Calor. for the High Energy Frontier (CHEF 2013)*, C13-04-22.4, p. 260.
13. http://geant4.cern.ch/support/userdocuments.shtml/PhysicsReferenceManual.pdf
14. A. Bolshakova et al. (HARP-CDP Group Collaboration), Eur. Phys. J. C **56**, 323 (2008); Eur. Phys. J. C **70**, 543 (2010).
15. B. Andersson et al., Nucl. Phys. B **281**, 289 (1987).
16. B. Nilsson-Almquist and E. Stenlund, Comp. Phys. Comm. **43**, 387 (1987).
17. A. S. Galoyan and V. V. Uzhinsky, EPAN Lett. **12**(1), 231 (2015) [Phys. Part. Nucl. Lett. **12**(1), 166 (2015)].
18. Kh. Abdel-Waged and V. V. Uzhinsky, Yad. Fiz. **60**, 925 (1997) [Phys. Atom. Nucl. **60**, 828 (1997)].
19. Kh. Abdel-Waged and V.V. Uzhinsky, J. Phys. G **24**, 1723 (1997).
20. Kh. Abdel-Waged and N. Felemban, Phys. Rev. C **91**, 034908 (2015).
21. M. I. Adamovich et al. (EMU-01 Collaboration), Zeit. fur Phys. A **358**, 337 (1997).
22. Kh. Abdel-Waged, N. Felemban, and V. V. Uzhinskii, Phys. Rev. C **84**, 014905 (2011).
23. A. Bolshakova et al. (HARP-CDP Group Collaboration), Eur. Phys. J. C **62**, 293 (2009); C **62**, 697 (2009); C **70**, 573 (2010); C **64**, 181 (2009); C **63**, 549 (2009).
24. A. Y. Abul-Magd, W. A. Friedman, and J. Hufner, Phys. Rev. C **34**, 113 (1986).
25. V. I. Yurevich, R. M. Yakovlev, and V. G. Lyapin, Phys. Atom. Nucl. **75**, 192 (2012) [Yad. Fiz. **75**, 214 (2012)].
26. V. I. Yurevich, R. M. Yakovlev, and V. G. Lyapin, Phys. Atom. Nucl. **69**, 1496 (2006) [Yad. Fiz. **69**, 1531 (2012)].